



Published in final edited form as:

Invest Ophthalmol Vis Sci. 2007 September ; 48(9): 4107–4115. doi:10.1167/iov.07-0080.

Bimatoprost, Prostanamide Activity and Conventional Drainage

Z. Wan^a, D.F. Woodward^c, C. Cornell^d, H. Fliri^d, J. Martos^d, S. Petit^d, J.W. Wang^c, A.B. Kharlamb^c, L.A. Wheeler^c, M.E. Garst^e, K. Landsverk^f, C.S. Struble^f, and W.D. Stamer^{a,b}

^aDepartment of Ophthalmology and Vision Science, the University of Arizona, Tucson, AZ ^bDepartment of Pharmacology, the University of Arizona, Tucson, AZ ^cDepartment of Biological Sciences Allergan, Inc., Irvine, CA, USA ^dDepartment of Chemistry, Selcia Ltd., Ongar, Essex, England ^eDepartment of Chemical Sciences Allergan, Inc., Irvine, CA, USA ^fCovance Inc., Madison, WI, USA.

Abstract

Purpose: Despite structural similarity with prostaglandin F_{2α}, the ocular hypotensive agent, bimatoprost (Lumigan), shows unique pharmacology in vitro and functional activity in vivo. Unfortunately, the precise mechanisms that underlie bimatoprost's distinctive impact on aqueous humor dynamics are unclear. The purpose of the current study was to investigate the effects of bimatoprost and a novel prostanamide-selective antagonist, AGN 211334, on human conventional drainage.

Methods: Two model systems were employed to test the consequences of bimatoprost and/or AGN 211334 treatment on conventional drainage. Human anterior segments in organ culture were perfused at a constant flow rate of 2.5 μl/min while pressure was recorded continuously. After stable baseline facilities were established, segments were treated with drug(s) and pressure was monitored for an additional three days. In parallel, drug(s) effects on hydraulic conductivity of human trabecular meshwork (TM) cell monolayers were evaluated. Pharmacological properties of AGN 211334 were characterized using isolated feline iris preparations in organ culture and heterologously expressed G-protein coupled receptors in vitro.

Results: Bimatoprost increased outflow facility by an average of 40 ± 10 % within 48 hours of treatment (n=10, p<0.001). Preincubation or coincubation with AGN 211334 significantly blunted bimatoprost effects by 95% or 43%, respectively. Similar results were obtained in cell culture experiments where bimatoprost increased hydraulic conductivity of TM cell monolayers by 78 ± 25 %. Pretreatment with AGN 211334 completely blocked bimatoprost effects while coincubation decreased bimatoprost effects on average by 74%. Interestingly, in both models AGN 211334 alone significantly decreased fluid flux across trabecular tissues/cells.

Conclusions: Our findings indicate that bimatoprost interacts with a prostanamide receptor in the trabecular meshwork to increase outflow facility.

Keywords

aqueous humor; organ culture; prostaglandin; Schlemm's canal; trabecular meshwork

Introduction

Glaucoma is a leading cause of adult blindness, affecting nearly 70 million people worldwide^{1, 2}. The most common form, primary open angle glaucoma is characterized by decreased outflow through the conventional drainage pathway that results in ocular hypertension³⁻⁵. Elevated intraocular pressure (IOP) over time appears to contribute to blindness by increasing mechanical stress on the optic nerve head, resulting in irreversible damage to retinal ganglion cell axons^{6, 7}.

Because of their efficacy at lowering IOP, prostaglandin (PG) compounds have been broadly used in clinical practice to treat ocular hypertension. The first PG mimetic used in the successful management of IOP was latanoprost, a synthetic PGF_{2α} analogue. Latanoprost is relatively inactive until its isopropyl ester is hydrolyzed to create a biologically active free acid that then functions as an FP receptor agonist⁸. Because of the efficacy of latanoprost, two additional mimetics, travoprost and unoprostone, have been developed for the treatment of ocular hypertension. The hypotensive activity of these three F_{2α} analogues seems to be accomplished by long-term remodeling of the extracellular matrix in the ciliary body^{9, 10}. Thus, the IOP lowering by PGs appears predominantly due to enhanced uveoscleral (unconventional) outflow¹¹.

Recently, a related PG compound, a prostamide called bimatoprost was introduced, and has proven to be an effective ocular hypotensive agents in patient studies¹²⁻¹⁴. Bimatoprost is synthetic molecule derived from anandamide that has structural and pharmacological similarity to PGF_{2α} ethanolamide. While structurally similar, evidence shows that bimatoprost possesses unique pharmacological and pharmacokinetic properties, distinct from known FP receptor agonists. For example, 1000 fold higher concentrations of bimatoprost than PGF_{2α} are required to induce [Ca²⁺]_i mobilization in cells that express endogenous FP receptors or cells that heterologously express human FP receptors^{14, 15}. Moreover, clinical pharmacological studies with bimatoprost reveal that, unlike latanoprost, bimatoprost is not significantly metabolized due to the absence of free acid hydrolysis product in systemic circulation after topical ocular administration to human volunteers^{16, 17}. The hydrolysis of bimatoprost to a free acid occurs at very low rate (<1% per hour) when exposed to a number of ocular and non-ocular tissues in three studies^{14, 16, 18} and at a higher rate in two other studies^{19, 20}. Lastly, bimatoprost fails to activate over 100 known drug targets, including a variety of receptors that may be involved in regulating IOP¹⁴. Unfortunately, because a prostamide receptor has not been cloned, their existence of is currently based on pharmacological criteria.

The mechanism by which prostamides differ from PG-F_{2α} agonists in their efficacy toward IOP regulation is still unknown. A recent study showed that bimatoprost treatment dampened the IOP rise due to water drinking in a group of glaucoma patients, suggesting an effect on the pressure-sensitive, conventional drainage pathway¹². In recent clinical studies, bimatoprost successfully lowered IOP in patients refractory to latanoprost therapy suggesting differences in the mechanism of action of prostamide and PGF_{2α}-receptor agonists^{13, 21}. Interestingly, in addition to changes observed in the extracellular matrix of the ciliary body, bimatoprost-treated monkeys displayed morphological changes in their conventional drainage pathway after one-year of treatment²². Taken together, these data suggest that bimatoprost has activity in the conventional drainage tract.

To specifically test the effects of bimatoprost on conventional drainage, we used the anterior segment perfusion model which preserves the architecture of the trabecular meshwork (TM) and allows the testing of conventional outflow function separately from unconventional function. To examine the role of prostamide receptors in control of conventional drainage, we tested the ability of a second generation prostamide-selective antagonist, AGN 211334, to

block bimatoprost effects. AGN 211334 is the latest compound in the series and is more than 10 times more potent than the prototypical prostamide antagonist AGN 204396²³. The presence of prostamide receptor activity in human TM cells was tested by recording changes in hydraulic conductivity of primary cultures of TM cell monolayers upon bimatoprost/AGN 211334 treatments. Results show that bimatoprost interacts with prostamide receptors on TM cells to increase outflow facility in situ and hydraulic conductivity in vitro.

Methods

Materials

Bimatoprost was synthesized by Allergan Incorporated (Irvine, CA). AGN 211334 was designed and synthesized by Selcia Ltd (Ongar, England). Stock solutions were prepared by dissolving drugs in ethanol giving a stock concentration of 10^{-3} M for bimatoprost and 3×10^{-3} M for AGN 211334 that were kept at -20°C until use. Stock solutions of isoproterenol (10^{-2} M, Calbiochem, La Jolla, CA) were made fresh in perfusion medium. Final solutions were prepared fresh by diluting stock solutions in perfusion medium immediately prior to chamber exchanges.

Anterior Segment Perfusion Model

Post mortem human eyes were obtained fresh from the National Disease Research Interchange (Philadelphia, PA) and Donor Network of Arizona (Phoenix, AZ). Eyes were free of any known ocular disease, and were stored in moistened chambers at 4°C until dissected. Preparation and perfusion of anterior segments were performed exactly as previously described by our laboratory; slightly modifying original descriptions of perfusion methods²⁴⁻²⁷. After dissection and mounting into culture chambers, anterior segments were perfused at a constant flow rate of $2.5 \mu\text{l}/\text{min}$ with Dulbecco's Modified Eagle's medium (DMEM) to which antibiotics (penicillin 100 U/ml, streptomycin 100 $\mu\text{g}/\text{ml}$ Sigma-Aldrich), bovine serum albumin (BSA) 25 mg/dl and 1% fetal bovine serum (FBS) were added. The anterior segments were cultured at 37°C in humidified air containing 5% CO_2 . Intrachamber pressures were continuously recorded with dedicated pressure transducers that interfaced with a digital data recorder and computer.

When stable baseline facilities were reached (typically after 2-4 days of perfusion), medium in anterior segments was exchanged under approximately 10 mmHg (13.6 cm H_2O) of constant pressure with medium containing 1 μM bimatoprost. We chose this concentration based upon ciliary body and iris tissue concentrations of bimatoprost observed in topically dosed non-human primates²⁸ and from preliminary studies in which we performed sequential dose-response exposures (10 nM-1 μM) and obtained consistent results only at 1 μM (not shown). Contralateral segments were exchanged with 30 μM AGN 211334 plus 1 μM bimatoprost (protocol 1) or 30 μM AGN 211334 alone and then were constantly perfused with drug solution. Anterior segments that initially received AGN 211334 were exchanged with medium containing 30 μM AGN 211334 plus 1 μM bimatoprost after 24 hours of pretreatment (protocol 2) and then were constantly perfused with drug solution. Forty-eight hours after initial drug treatments, medium from anterior segment pairs was exchanged with fresh medium without drug(s), and segments were perfused for an additional 3-4 days.

Central Corneal Thickness

The SP-100 Handy Pachymeter (Tomey Corporation, Japan) was used to obtain central corneal thickness (CCT) measurements of whole globes upon arrival to our laboratory and anterior segments during perfusion²⁷. After initial measurements on whole globes, CCT was measured on anterior segments 2 hours after the start of perfusion, and every 24 to 48 hours afterwards²⁷. Data points were the average of three readings taken sequentially. If one of the readings

was significantly different from the other two (>100 μ m), two more readings were made, and both the highest and the lowest were discarded. The slope was calculated from the CCT measurements obtained after the start of perfusion to the day of the first of drug treatment(s).

Morphological Analysis

At the end of perfusion, medium in anterior chambers was exchanged with 3% paraformaldehyde (PFA) in phosphate-buffered saline (pH 7.4) under 10 mmHg pressure. After perfusion at 2.5 μ l/min for 1 hour with PFA, anterior segments were removed from culture chambers and several wedges (~2 mm wide) containing outflow tissues were cut from each of four quadrants using a #15 scalpel blade and were stored in 2% PFA. Representative wedges from each quadrant were embedded in Spurr's plastic according to standard methods and stained with toluidine blue²⁶. Sagittally oriented 0.5 μ m sections were viewed by light microscopy using an Olympus BH-2 upright microscope at magnifications of 200x and 400x. All sections were evaluated in a masked fashion by two observers according to a grading scheme that was described previously²⁷.

0= no cells in the trabecular meshwork (TM) or only a few swollen cells; inner wall disruption (breaks, other damage) present

1= only a few cells in the TM, typically in the juxtacanalicular tissue (JCT), but existing cells show little or no swelling, inner wall intact

2= JCT well populated with cells; corneoscleral and uveal meshworks contain few or no cells; inner wall intact

3= JCT and most of corneoscleral meshwork filled with cells; most cells look good (no swelling); inner wall intact

4= trabecular meshwork looks essentially normal; cells are present everywhere in the JCT and corneoscleral meshwork (uveal mesh not considered); inner wall intact.

The final reported grade for each anterior segment was calculated by averaging the scores of all four quadrants in an anterior segment from two observers (Table 2).

Cell Culture

Three previously characterized strains of human trabecular meshwork cells (HTM 61, 86, and 89) were used in the present study^{29, 30}. HTM cells were cultured in Dulbecco's Modified Eagle Medium (low glucose DMEM; Gibco, Carlsbad, CA), and supplemented with 10% Fetal Bovine Serum (Gemini, Woodland, CA) and 100U/ml penicillin, 0.1mg/ml streptomycin, and 0.29 mg/ml glutamine (Invitrogen, San Diego, CA) and grown in humidified air containing 5% CO₂ at 37°C. Cells (1×10^5) were seeded onto polycarbonate membrane filters (tissue culture treated, 12mm diameter 0.4 μ m pore size; Corning Incorporated, Corning, NY) at confluence and allowed 9-12 days for monolayers to mature before experimentation.

Cell Perfusions

Filters with cells were placed into an Ussing-type chamber filled with HEPES-buffered DMEM (25mM HEPES, pH 7.4). The chamber, tubing, and reservoir were gently filled with DMEM + HEPES and the cells were allowed to acclimate for 30 minutes at 37°C with no pressure gradient. To start the experiment, the reservoir was raised to 13.6 cm above the midline of the filter containing cells (giving a 10 mmHg pressure differential across the cells) and allowed to perfuse for 30 minutes at 37°C, giving initial baseline measurement. Afterwards, the chamber was exchanged with fresh medium containing 1 μ M Isoproterenol, 1 μ M Bimatoprost, and/or 30 μ M AGN 211334. The cell monolayers were again exposed to a pressure head of 10 mmHg for 30 minutes and hydraulic conductivity was recorded^{31, 32}. Experiments were concluded

by removing the filters from the chamber, rinsing cells twice in phosphate-buffered saline and fixing cells with 4% paraformaldehyde in PBS. For inclusion of the data, initial hydraulic conductivity measurements (both before and after mock exchange) must have been stable, (i.e.: within 5% of each other) and in the span of 1.5-6 $\mu\text{L}/\text{min}/\text{mmHg}/\text{cm}^2$ such that drug-induced changes relative to the baseline would remain in the range of detection for the force displacement transducer.

Feline Iris Contraction Model

Feline iris sphincter tissues prepared as described previously were mounted vertically under 50 to 100 mg tension in a jacketed 10 ml organ bath³³. Smooth muscle tension of the isolated iris sphincter was measured isometrically with force displacement transducers (Grass FT-03) and recorded on a Grass polygraph (Model 7). The organ baths contained Krebs' solution maintained at 37°C by a heat exchanger and circulating pump. The Krebs' solution (118.0 mM NaCl, 4.7 mM KCl, 1.2 mM KH_2PO_4 , 1.9 mM CaCl_2 , 1.18 mM MgSO_4 , 25.0 mM NaHCO_3 , 11.7 mM glucose and 0.001 mM indomethacin) was gassed with 95% O_2 , 5% CO_2 to give a pH of 7.4. Tissues were allowed 60 min to stabilize before commencing each experiment. The feline iris experiments were designed so that a direct, four-way comparison for antagonist vs. prostamide, vehicle vs. prostamide, antagonist vs. corresponding PG, and vehicle vs. corresponding PG was provided in tissue preparations obtained from a single animal. One cumulative dose-response curve to agonist was obtained in each tissue. Vehicle (ethanol) and antagonist (AGN 211334) were given 30 minutes before the agonist dose-response curves were constructed. The response to $\text{PGF}_{2\alpha}$ 10^{-7}M was determined at the beginning and end of each dose response curve, with appropriate wash-out, and responses were calculated as % of this reference contraction.

Ca^{2+} Signal Studies on Human Recombinant Prostanoid Receptors

The use of chimeric G protein cDNAs (prostanoid DP, EP_1 , EP_2 , EP_4 , FP, IP and TP) stably expressed in HEK-293 EBNA cells allowed responses to G_s and G_i coupled prostanoid receptors to be measured as a Ca^{2+} signal, as previously described³³. Ca^{2+} signaling studies were performed using a FLIPR (fluorometric imaging plate reader) instrument. Cells were seeded at a density of 5×10^4 cells/well in Biocoat poly-D-lysine coated, black wall, clear bottom 96 well plates (BD Biosciences, Franklin Lakes, NJ) and allowed to attach overnight in an incubator at 37°C. The cells were then washed twice with HBSS-HEPES buffer (Hanks' balanced salt solution without bicarbonate and phenol red, 20 mM HEPES, pH 7.4) using a Denley Cellwash plate washer (Labsystems, Franklin, MA). After 45-60 min of dye-loading in the dark using the Ca^{2+} -sensitive dye Fluo-4AM, at a final concentration of $2 \times 10^{-6}\text{M}$, the plates were washed 4 times with HBSS-HEPES buffer to remove excess dye and leaving 100 μl of buffer in each well. The plates were then placed in the FLIPR instrument and allowed to equilibrate at 37°C. Compound solutions were added in a 50 μl volume to each well to give the desired final concentration. Cells were excited with an argon laser at 488 nm and emission was measured through a 510-570 nm band width emission filter (FLIPR, Molecular Devices, Sunnyvale, CA). The peak increase in fluorescence intensity was recorded for each well.

The experimental design for the FLIPR studies was as follows. On each plate, four wells each served as negative (HBSS-HEPES buffer) and positive controls (standard agonist: DP = BW 245C, EP_1 - EP_4 = PGE_2 , FP = $\text{PGF}_{2\alpha}$, IP = carbaprostacyclin TP=U-46619). The peak fluorescence change in each well containing drug was expressed relative to the controls. To obtain concentration-response curves, compounds were tested in duplicate in each plate over the desired concentration range. Each compound was tested on at least 3 separate plates using cells from different passages to give n=3.

Statistical Analysis

Drug effects were expressed as the percentage increase or decrease in outflow facility (or hydraulic conductivity) after drug administration (Cd) compared to baseline (Co) and calculated as $(Cd-Co)/Co \times 100\%$. A paired two sample *t*-test was performed for statistical analysis. P values less than 0.01 were considered as statistically significant. For anterior segment perfusions, the Co was the mean of facility that stable for at least 24 hours before any treatment. Cd was the mean facility of the second 12 hour after each treatment day. Washout facility was the mean facility of the second 12 hours after washout. Values were expressed as the mean \pm SEM.

Results

AGN 211334 Blockade in Feline Iris

The structures of bimatoprost, a prostamide antagonist AGN 211334, prostamide $F_{2\alpha}$ and $PGF_{2\alpha}$ are shown in figure 1A. To examine the specificity of AGN 211334 as an antagonist, effects of AGN 211334 (30 μ M) on contractions produced by bimatoprost, prostamide $F_{2\alpha}$ and PG- $F_{2\alpha}$ are shown in figure 1B, 1C and 1D. AGN 211334 produced a clear right shift of the bimatoprost concentration-response curve (10^{-10} M- 10^{-5} M, figure 1B) and a clear rightward shift of the prostamide $F_{2\alpha}$ concentration-response curve (10^{-9} M- 10^{-5} M, figure 1C) as well, but no significant shift of the $PGF_{2\alpha}$ concentration-response curve (figure 1D) in feline iris preparations.

AGN 211334 blockade at Human Recombinant Prostanoid Receptors.

The effects of a 30 μ M concentration of AGN 211334 on Ca^{2+} signals associated with human recombinant prostanoid receptor activation are summarized in Table 1. Antagonism was not apparent at DP, EP₁, EP₂, EP₃, EP₄, FP or IP receptors but AGN 211334 was an efficacious TP receptor antagonist ($K_b=16$ nM). This data is compared in table 1 with the K_b value obtained for AGN 211334 vs. prostamide $F_{2\alpha}$ in the isolated feline iris, as previously described (42).

Bimatoprost and AGN211334 Effects on Outflow Facility

Perfused human anterior segments in organ culture were used to assess the effects of bimatoprost and AGN211334 on conventional outflow function. Twenty anterior segments from 11 donors were examined. Age of donors ranged from 49-91 (mean: 67.5 \pm 3.5 years), average time from death to enucleation was 6.3 \pm 1.1 hrs, while mean time from death to perfusion was 34.6 \pm 1.6 hours (Table 2).

To examine effects of bimatoprost on conventional drainage, two experimental paradigms were used: In the first, one anterior segment from a pair with stable outflow facilities was treated with bimatoprost, while the contralateral segment was exposed to bimatoprost (1 μ M) plus AGN 211334 (30 μ M). In the second protocol, one segment of the pair was treated with bimatoprost, while the other was first pretreated with AGN 211334 and then 24 hours later was treated with bimatoprost plus AGN 211334. Examples of traces from anterior segments that were subjected to the two protocols are shown in figure 2. In both traces bimatoprost effects are immediate and steady over the two days of exposure (black traces). Upon washout of bimatoprost with fresh perfusion medium, we observed two types of responses, either facility stabilized at a level higher than original baseline (panel B, n=5) or continued to increase (panel A, n=5), but at a more gradual rate. We compared the slope of facility increase during bimatoprost treatment (0.03 \pm 0.01) versus slope of increase after washout (0.01 \pm 0.01), and found them to be different (p=0.02). In contrast, outflow facility of all anterior segments treated with bimatoprost and AGN 211334 concurrently increased at a rate lower than bimatoprost treatment alone (panel A). Outflow facility of all anterior segments *pretreated* with AGN

211334 before co-treatment with bimatoprost remained similar to initial baseline measurements (panel B).

A summary of outflow facility responses to drug treatments are shown in figure 3. Ten anterior segments were exposed to bimatoprost with an average starting (baseline) facility of $0.18 \pm 0.04 \mu\text{l}/\text{min}/\text{mm Hg}$ (Table 3). When expressed as percentage change from baseline, the average facility increase for the 10 segments was 14% after 24 hours ($p=0.001$), and 40% after 48 hours ($p=0.0002$). After washout, outflow facility continued to increase, but at a slower rate; reaching a maximum of 49% seventy two hours following initial exposure to bimatoprost ($p=0.001$). The mean starting facility of 4 contralateral anterior segments co-treated with AGN 211334 plus bimatoprost was $0.24 \pm 0.09 \mu\text{l}/\text{min}/\text{mm Hg}$ (Table 3). The average increase in facility was 6% after 24 hours ($p=0.02$) and 23% after 48 hours ($p=0.03$). Following washout, outflow facility on average was 17% higher than original baseline, but not significantly different ($p=0.3$). The average baseline outflow facility of 6 fellow segments pre-treated with AGN 211334 alone was $0.15 \pm 0.02 \mu\text{l}/\text{min}/\text{mm Hg}$ (Table 3). Upon exposure of trabecular tissues to AGN 211334, outflow facility decreased by 4% after 24 hours ($p=0.04$). Addition of bimatoprost to AGN-pretreated segments increased outflow facility by 2% above initial baseline ($p=0.3$). Following a chamber exchange with fresh medium, average outflow facility in AGN-pretreated segments measured 1% lower than original baseline ($p=0.5$). Shown in figure 4 are representative images of histological sections taken from an anterior segment pair that was treated with bimatoprost (panel A) or bimatoprost following pre-treatment with AGN 211334 (panel B).

Bimatoprost and Central Corneal Thickness

In addition to post-perfusion evaluation of conventional outflow tissues by standard histology, CCT slope and outflow facility were two functional measurements in the present study used to assess the quality of anterior segment tissues during perfusion (Table 2)²⁷. The rate of CCT recovery was calculated as rate of change of corneal thickness over the first three days of perfusion ($\mu\text{m}/\text{hour}$). On average, the CCT of the 20 anterior segments tested decreased by $1.4 \mu\text{m}/\text{hour}$ over the first three days of perfusion (Table 1).

After administering drugs, we continued to measure CCT on all anterior segments. Interestingly, we observed that compared to initial measurements, CCT increased in 8 out of 10 segments receiving bimatoprost alone. Shown in figure 5, the average CCT for the bimatoprost alone group was $778 \pm 37 \mu\text{m}$ immediately before treatment, and increased to $832 \pm 37.1 \mu\text{m}$ two days after treatment ($p=0.015$). The CCT returned to an average of $784 \pm 56.8 \mu\text{m}$ two days after chamber exchange ($P=0.4$). In contrast, anterior segments pretreated with AGN 211334 had no significant changes in CCT following drug(s) treatment. The average CCT was $752 \pm 49 \mu\text{m}$ before treatment and $762 \pm 58 \mu\text{m}$ two days after treatment ($p=0.3$) and $755 \pm 62 \mu\text{m}$ ($p=0.5$) two days after wash.

Bimatoprost and AGN 211334 Effects on TM Monolayers

To determine whether bimatoprost's molecular target in the conventional drainage tract resides on trabecular meshwork cells, we examined the effects of bimatoprost on hydraulic conductivity (HC) across mature monolayers of human TM cells in culture. Panel A of figure 6 shows that bimatoprost ($1 \mu\text{M}$) increased HC of TM monolayers by $78 \pm 25\%$ and $75\% \pm 23\%$, respectively in two successive treatments ($p \leq 0.01$). As a positive control for this model, panel B demonstrates that isoproterenol ($1 \mu\text{M}$) significantly increased HC in two successive treatments as shown previously by others³¹. However, panels C and D show that when used in combination, effects of isoproterenol and bimatoprost were not additive or synergistic. To determine specificity of AGN 211334 on bimatoprost effects in this third model system, cell monolayers were either *preincubated* or *coincubated* with antagonist. Similar to results

obtained in perfused human anterior segments, AGN 211334 (30 μ M) partially antagonized bimatoprost effects when introduced to cells together (panel E) and totally blocked bimatoprost effects if cells were pretreated (panel F). Interestingly, when TM cells were exposed to AGN 211334 alone, fluid flow across trabecular cells significantly decreased by $51 \pm 0.8\%$ ($p < 0.001$, panel F).

Discussion

Our findings provide, for the first time, direct evidence that bimatoprost interacts with cells of the conventional drainage pathway to increase outflow facility. Such effects were attenuated significantly by pretreatment or co-administration with the prostamide-specific antagonist, AGN 211334. Prostamide receptors appear to be located on trabecular meshwork cells because AGN 211334 effectively blocked bimatoprost-induced increases in hydraulic conductivity of TM cell monolayers. Collectively, these results suggest that in addition to effects shown previously on uveoscleral outflow, bimatoprost working through prostamide receptors, increases conventional outflow.

To test our hypothesis that bimatoprost affects conventional drainage, fresh human anterior segments in organ culture were utilized, providing several advantages over other model systems. First, the architecture and cellular relationships in the conventional drainage tract are preserved; Second, the anterior segment allows for long term study of drug effects, enabling multiple manipulations (e.g.: sequential drug treatments) to occur over the lifetime of the experiment^{34, 35}; Third, the conventional drainage pathway in humans differs from other species, including non-human primates, in terms of micro and gross anatomy³⁶⁻³⁸; Lastly and most relevant to the present study, nonhuman primates seem to differ from humans with respect to bimatoprost effects on outflow facility. Thus, bimatoprost appears to increase conventional and unconventional outflow facility in humans, but only unconventional in monkeys^{14, 39}.

The cellular target (receptor) for bimatoprost has been controversial. Some argue that bimatoprost is a prostaglandin $F_{2\alpha}$ pro-drug, like lantanoprost, which upon application to the eye is hydrolyzed and behaves as a FP receptor agonist^{19, 20}. In fact, when hydrolyzed in the test tube, the free-acid of bimatoprost potentially activates FP receptors¹⁵. However, in some studies bimatoprost appears to be highly resistant to hydrolysis and thus the appearance of the free acid of bimatoprost is rare in ocular tissues, particularly in regions such as ciliary body thought to primarily mediate outflow effects^{19, 40}. Other evidence suggests that $PGF_{2\alpha}$ and bimatoprost interact at different receptors. When tested in the same tissue preparation, $PGF_{2\alpha}$ and bimatoprost stimulate calcium transients in different cell populations^{41, 42} and differentially stimulate connective tissue growth factor⁴³. Lastly, bimatoprost shows no meaningful activity at prostaglandin FP receptors or other PG receptor subtypes ($K_d \geq 10^{-5}$ M)^{16, 33}.

In our hands, AGN 211334 effectively blocks bimatoprost, prostamide $F_{2\alpha}$, but not $PGF_{2\alpha}$ -mediated contractions. Additionally, in both of our models for the conventional pathway, AGN 211334 antagonized prostamide (bimatoprost) effects on fluid flow through trabecular tissues and across trabecular monolayers. Interestingly, AGN 211334 alone decreased baseline outflow facility measurements in perfused anterior segment and initial hydraulic conductivity measurements for TM cell monolayers, suggesting that AGN 211334 interferes with endogenous signaling pathways or acts as an inverse agonist in these preparations. Due to potent and reproducible effects of AGN 211334 on hydraulic conductivity of TM cell monolayers, this model will serve as a useful tool to uncover the mechanism of AGN 211334 action in future studies.

Bimatoprost has proven to be a safe and effective agent for lowering IOP in the management of ocular hypertension and open-angle glaucoma. In the present study we observed that bimatoprost treatment adversely affected CCT measurements; effects that were antagonized by AGN 211334. To our knowledge, corneal edema has not been reported during clinical trials with bimatoprost. A recent study indicated that other antiglaucoma drugs including latanoprost may affect the physiologic function of corneal endothelial cells through change of $[Ca^{2+}]_i$ mobility⁴⁴. The effect of bimatoprost on the corneal endothelium is still unclear and requires further characterization.

In clinical studies bimatoprost appears to affect IOP earlier than other prostaglandin mimetics and effects are long lasting. Bimatoprost demonstrated effective 24-hr IOP control after a single dose in both human and normal dogs, and almost 10 mmHg was dropped 4 hours after a single dose in glaucomatous dogs¹⁴. In the anterior segment perfusion model used in the current study, bimatoprost gradually increased outflow facility over the two days of exposure and continued to increase outflow facility in some segments after chamber exchange with fresh medium (probably because of difficulty in washing bimatoprost out of tissues). Consistent with this finding, careful examination of outflow tissues exposed to bimatoprost with the light microscope revealed no consistent morphological changes (i.e.: breaks in inner wall, not shown). In contrast, bimatoprost effects in the cell perfusion model were observed immediately, during the first 30 minutes of exposure. Because bimatoprost effects were not additive or synergistic with isoproterenol, we concluded that both drugs were affecting intracellular pathways that control cell contractility as shown before³¹. The reasons for the time differences between the models are unclear. However, in both cases effects appeared sooner than would be anticipated if bimatoprost was influencing remodeling of extracellular matrix in juxtacanalicular tissues or in cell monolayers. Alternatively, bimatoprost may have two mechanisms of action; one that occurs immediately and another that occurs over time. For example, we cannot rule out that bimatoprost alters the extracellular matrix environment in the conventional drainage tract and/or the sclera, similar to effects of $PGF_{2\alpha}$ and its analogues⁴⁵. Clearly, more work needs to be done to characterize bimatoprost effects in the outflow tracts.

The unique pharmacology of bimatoprost and its effects on conventional drainage provide a lead compound to dissect out mechanisms that regulate resistance to outflow in the conventional drainage tract. Understanding these mechanisms will enable the design of more efficacious compounds with the ability to increase conventional outflow in those afflicted with ocular hypertension and glaucoma.

Acknowledgments

The authors thank Serena Coons for her excellent technical assistance with cell perfusion experiments, Renata Ramos for scoring histology sections and Kristin Perkumas for careful editing of manuscript.

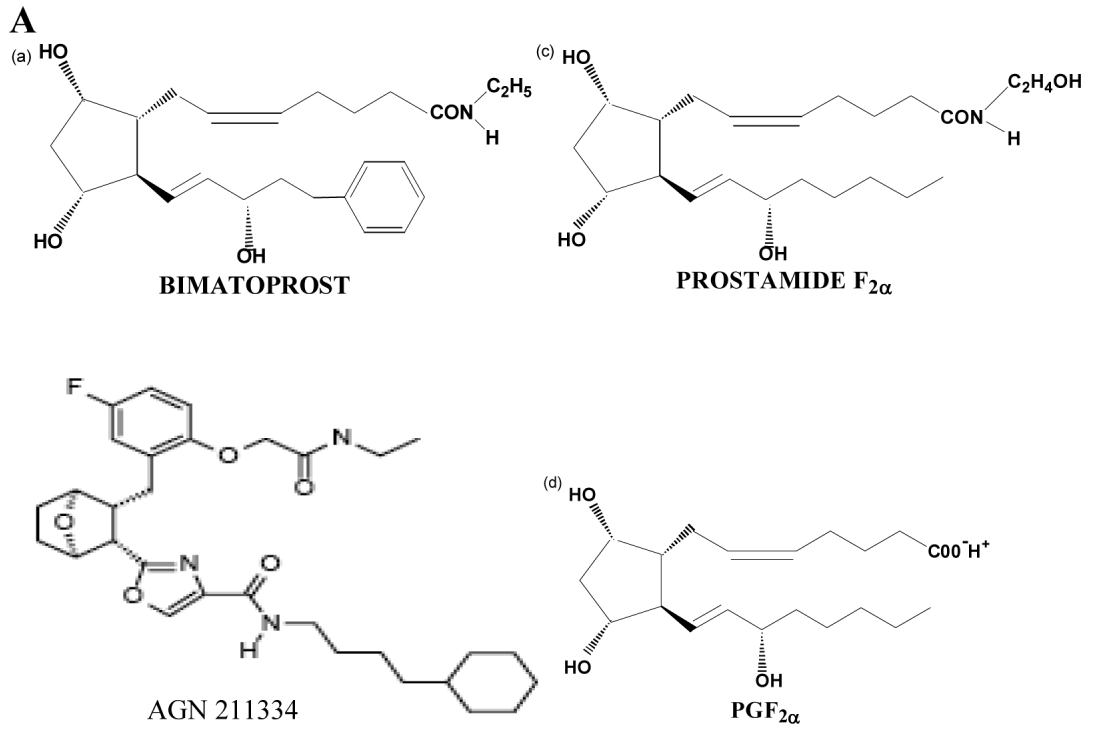
Supported in part through a grant from the National Eye Institute (EY12797) and career development award to WDS from Research to Prevent Blindness Foundation.

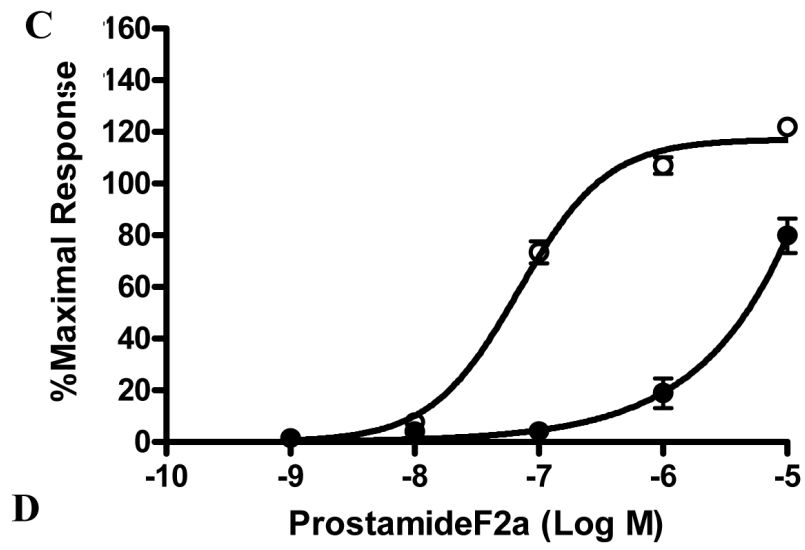
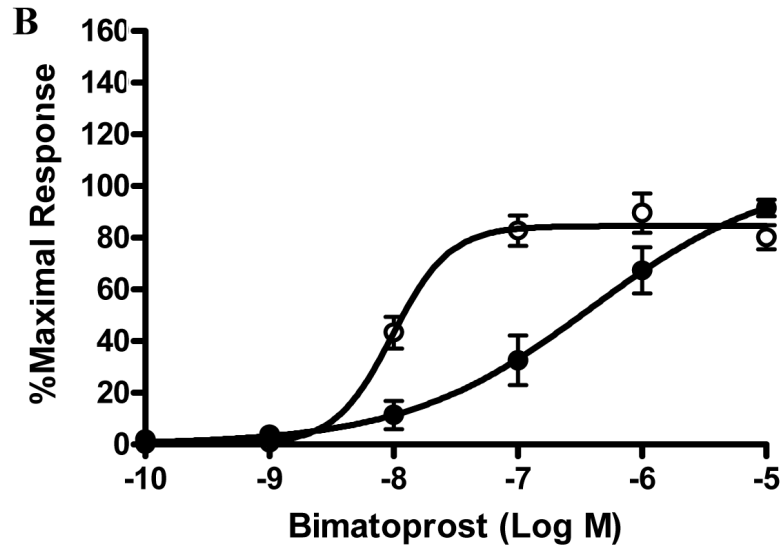
Reference

1. Leske MC. The epidemiology of open-angle glaucoma: a review. *Am J Epidemiol* 1983;118:166–91. [PubMed: 6349332]
2. Quigley HA. Number of people with glaucoma worldwide. *Br J Ophthalmol* 1996;80:389–93. [PubMed: 8695555]
3. Alvarado J, Murphy C, Juster R. Trabecular meshwork cellularity in primary open-angle glaucoma and nonglaucomatous normals. *Ophthalmology* 1984;91:564–79. [PubMed: 6462622]

4. Lutjen-Drecoll E, Futa R, Rohen JW. Ultrahistochemical studies on tangential sections of the trabecular meshwork in normal and glaucomatous eyes. *Invest Ophthalmol Vis Sci* 1981;21:563–73. [PubMed: 7287346]
5. Rohen JW. Why is intraocular pressure elevated in chronic simple glaucoma? Anatomical considerations. *Ophthalmology* 1983;90:758–65. [PubMed: 6413918]
6. Lutjen-Drecoll E. Morphological changes in glaucomatous eyes and the role of TGFbeta2 for the pathogenesis of the disease. *Exp Eye Res* 2005;81:1–4. [PubMed: 15978248]
7. Morrison JC, Johnson EC, Cepurna W, Jia L. Understanding mechanisms of pressure-induced optic nerve damage. *Prog Retin Eye Res* 2005;24:217–40. [PubMed: 15610974]
8. Hylton C, Robin AL. Update on prostaglandin analogs. *Curr Opin Ophthalmol* 2003;14:65–9. [PubMed: 12698043]
9. Lindsey JD, Kashiwagi K, Kashiwagi F, Weinreb RN. Prostaglandins alter extracellular matrix adjacent to human ciliary muscle cells in vitro. *Invest Ophthalmol Vis Sci* 1997;38:2214–23. [PubMed: 9344344]
10. Weinreb RN, Lindsey JD. Metalloproteinase gene transcription in human ciliary muscle cells with latanoprost. *Invest Ophthalmol Vis Sci* 2002;43:716–22. [PubMed: 11867589]
11. Weinreb RN, Toris CB, Gabelt BT, Lindsey JD, Kaufman PL. Effects of prostaglandins on the aqueous humor outflow pathways. *Surv Ophthalmol* 2002;1(47 Suppl):S53–64. [PubMed: 12204701]
12. Christiansen GA, Nau CB, McLaren JW, Johnson DH. Mechanism of ocular hypotensive action of bimatoprost (Lumigan) in patients with ocular hypertension or glaucoma. *Ophthalmology* 2004;111:1658–62. [PubMed: 15350319]
13. Gandolfi SA, Cimino L. Effect of bimatoprost on patients with primary open-angle glaucoma or ocular hypertension who are nonresponders to latanoprost. *Ophthalmology* 2003;110:609–14. [PubMed: 12623831]
14. Woodward DF, Krauss AH, Chen J, et al. The pharmacology of bimatoprost (Lumigan). *Surv Ophthalmol* 2001;4(45 Suppl):S337–45. [PubMed: 11434936]
15. Sharif NA, Williams GW, Kelly CR. Bimatoprost and its free acid are prostaglandin FP receptor agonists. *Eur J Pharmacol* 2001;432:211–3. [PubMed: 11740958]
16. Woodward DF, Phelps RL, Krauss AH, et al. Bimatoprost: a novel antiglaucoma agent. *Cardiovasc Drug Rev* 2004;22:103–20. [PubMed: 15179448]
17. Woodward DF, Krauss AH, Chen J, et al. Replacement of the carboxylic acid group of prostaglandin f(2alpha) with a hydroxyl or methoxy substituent provides biologically unique compounds. *Br J Pharmacol* 2000;130:1933–43. [PubMed: 10952685]
18. Sjoquist B, Stjernschantz J. Ocular and systemic pharmacokinetics of latanoprost in humans. *Surv Ophthalmol* 2002;1(47 Suppl):S6–12. [PubMed: 12204697]
19. Davies SS, Ju WK, Neufeld AH, Abran D, Chemtob S, Roberts LJ 2nd. Hydrolysis of bimatoprost (Lumigan) to its free acid by ocular tissue in vitro. *J Ocul Pharmacol Ther* 2003;19:45–54. [PubMed: 12648303]
20. Camras CB, Toris CB, Sjoquist B, et al. Detection of the free acid of bimatoprost in aqueous humor samples from human eyes treated with bimatoprost before cataract surgery. *Ophthalmology* 2004;111:2193–8. [PubMed: 15582073]
21. Williams RD. Efficacy of bimatoprost in glaucoma and ocular hypertension unresponsive to latanoprost. *Adv Ther* 2002;19:275–81. [PubMed: 12665048]
22. Richter M, Krauss AH, Woodward DF, Lutjen-Drecoll E. Morphological changes in the anterior eye segment after long-term treatment with different receptor selective prostaglandin agonists and a prostamide. *Invest Ophthalmol Vis Sci* 2003;44:4419–26. [PubMed: 14507888]
23. Woodward DF, Krauss AH, Wang JW, et al. Identification of an antagonist that selectively blocks the activity of prostamides (prostaglandin-ethanolamides) in the feline iris. *Br J Pharmacol*. 2006
24. Johnson DH, Tschumper RC. Human trabecular meshwork organ culture. A new method. *Invest Ophthalmol Vis Sci* 1987;28:945–53. [PubMed: 3583633]
25. Johnson DH, Tschumper RC. The effect of organ culture on human trabecular meshwork. *Exp Eye Res* 1989;49:113–27. [PubMed: 2759186]

26. Gottanka J, Chan D, Eichhorn M, Lutjen-Drecoll E, Ethier CR. Effects of TGF-beta2 in perfused human eyes. *Invest Ophthalmol Vis Sci* 2004;45:153–8. [PubMed: 14691167]
27. Wan Z, Brigatti L, Ranger-Moore J, Ethier CR, Stamer WD. Rate of change in central corneal thickness: a viability indicator for conventional drainage tissues in organ culture. *Exp Eye Res* 2006;82:1086–93. [PubMed: 16466713]
28. Woodward DF, Krauss AH, Chen J, et al. Pharmacological characterization of a novel antiglaucoma agent, Bimatoprost (AGN 192024). *J Pharmacol Exp Ther* 2003;305:772–85. [PubMed: 12606640]
29. Stamer WD, Roberts BC, Howell DN, Epstein DL. Isolation, culture, and characterization of endothelial cells from Schlemm's canal. *Invest Ophthalmol Vis Sci* 1998;39:1804–12. [PubMed: 9727403]
30. Stamer WD, Seftor RE, Williams SK, Samaha HA, Snyder RW. Isolation and culture of human trabecular meshwork cells by extracellular matrix digestion. *Curr Eye Res* 1995;14:611–7. [PubMed: 7587308]
31. Alvarado JA, Murphy CG, Franse-Carman L, Chen J, Underwood JL. Effect of beta-adrenergic agonists on paracellular width and fluid flow across outflow pathway cells. *Invest Ophthalmol Vis Sci* 1998;39:1813–22. [PubMed: 9727404]
32. Burke AG, Zhou W, O'Brien ET, Roberts BC, Stamer WD. Effect of hydrostatic pressure gradients and Na₂EDTA on permeability of human Schlemm's canal cell monolayers. *Curr Eye Res* 2004;28:391–8. [PubMed: 15512946]
33. Matias I, Chen J, De Petrocellis L, et al. Prostaglandin ethanolamides (prostamides): in vitro pharmacology and metabolism. *J Pharmacol Exp Ther* 2004;309:745–57. [PubMed: 14757851]
34. Erickson KA, Schroeder A. Direct effects of muscarinic agents on the outflow pathways in human eyes. *Invest Ophthalmol Vis Sci* 2000;41:1743–8. [PubMed: 10845594]
35. Crawford KS, Gange SJ, Gabelt BT, et al. Indomethacin and epinephrine effects on outflow facility and cyclic adenosine monophosphate formation in monkeys. *Invest Ophthalmol Vis Sci* 1996;37:1348–59. [PubMed: 8641838]
36. Overby D, Gong H, Qiu G, Freddo TF, Johnson M. The mechanism of increasing outflow facility during washout in the bovine eye. *Invest Ophthalmol Vis Sci* 2002;43:3455–64. [PubMed: 12407156]
37. Wang YL, Toris CB, Zhan G, Yablonski ME. Effects of topical epinephrine on aqueous humor dynamics in the cat. *Exp Eye Res* 1999;68:439–45. [PubMed: 10192801]
38. Wang RF, Lee PY, Taniguchi T, et al. Effect of oxymetazoline on aqueous humor dynamics and ocular blood flow in monkeys and rabbits. *Arch Ophthalmol* 1993;111:535–8. [PubMed: 8470989]
39. Brubaker RF. Measurement of uveoscleral outflow in humans. *J Glaucoma* 2001;10:S45–8. [PubMed: 11890274]
40. Maxey KM, Johnson JL, LaBrecque J. The hydrolysis of bimatoprost in corneal tissue generates a potent prostanoid FP receptor agonist. *Surv Ophthalmol* 2002;1(47 Suppl):S34–40. [PubMed: 12204699]
41. Chen J, Senior J, Marshall K, et al. Studies using isolated uterine and other preparations show bimatoprost and prostanoid FP agonists have different activity profiles. *Br J Pharmacol* 2005;144:493–501. [PubMed: 15678094]
42. Spada CS, Krauss AH, Woodward DF, et al. Bimatoprost and prostaglandin F(2 alpha) selectively stimulate intracellular calcium signaling in different cat iris sphincter cells. *Exp Eye Res* 2005;80:135–45. [PubMed: 15652534]
43. Liang Y, Li C, Guzman VM, et al. Comparison of prostaglandin F2alpha, bimatoprost (prostamide), and butaprost (EP2 agonist) on Cyr61 and connective tissue growth factor gene expression. *J Biol Chem* 2003;278:27267–77. [PubMed: 12724323]
44. Wu KY, Hong SJ, Wang HZ. Effects of antiglaucoma drugs on calcium mobility in cultured corneal endothelial cells. *Kaohsiung J Med Sci* 2006;22:60–7. [PubMed: 16568722]
45. Kim JW, Lindsey JD, Wang N, Weinreb RN. Increased human scleral permeability with prostaglandin exposure. *Invest Ophthalmol Vis Sci* 2001;42:1514–21. [PubMed: 11381055]





D

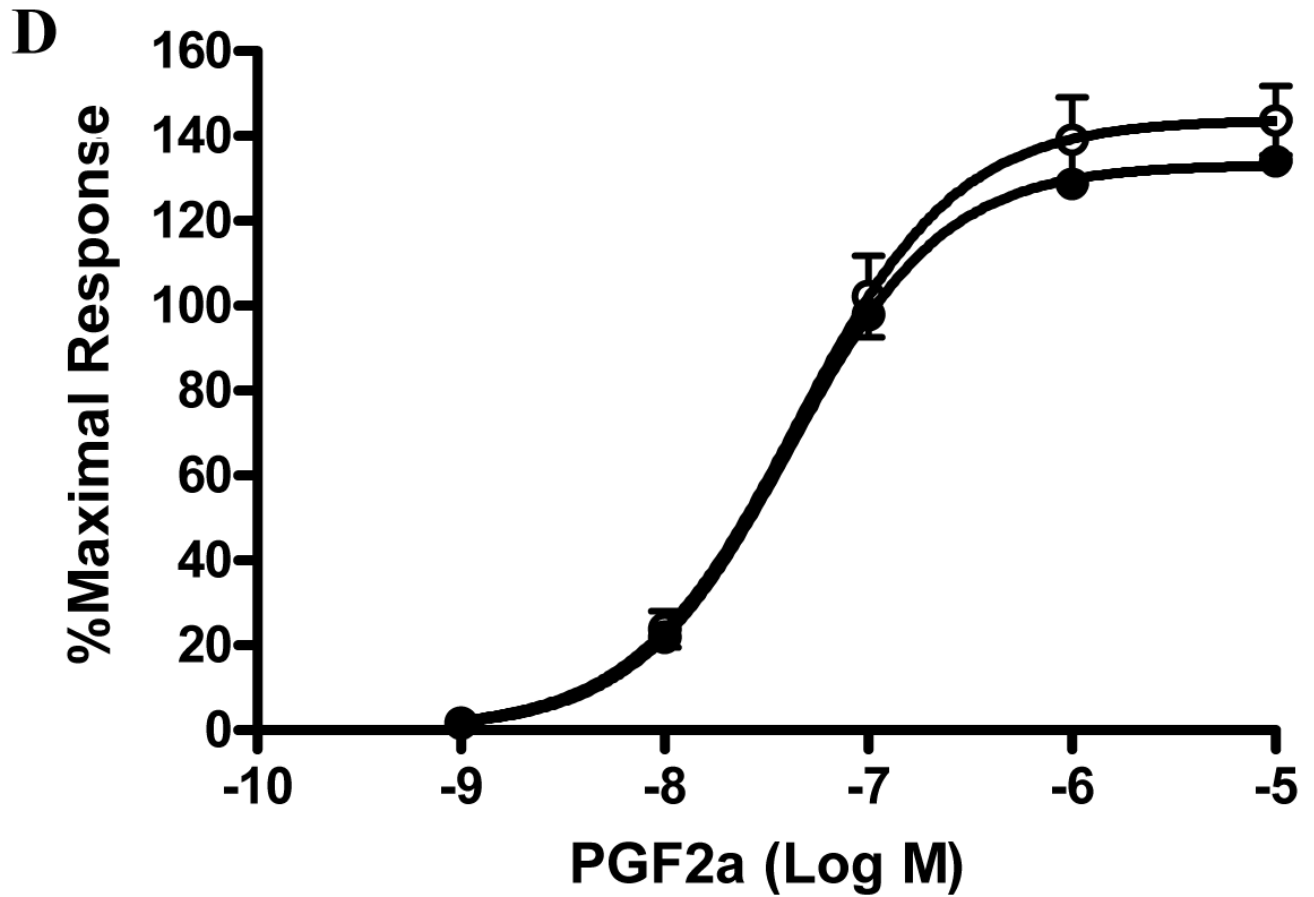


Figure 1. Specificity of the prostamide antagonist, AGN 211334

Chemical structures of bimatoprost, AGN 211334, prostamide $F_{2\alpha}$ and $PGF_{2\alpha}$ are shown in [panel A](#). Effects of the presence of AGN 211334 ($30\mu M$) on contraction of the feline iris produced by bimatoprost ([panel B](#)) prostamide $F_{2\alpha}$ ([panel C](#)) $PGF_{2\alpha}$ ([panel D](#)) are shown. Concentration-response curves are displayed for each agonist, either in the presence (●) or absence (○) of antagonist. Values shown are mean \pm SEM. AGN 211334 significantly changed EC_{50} value for bimatoprost and prostamide, but not prostaglandin $F_{2\alpha}$ ($p < 0.01$).

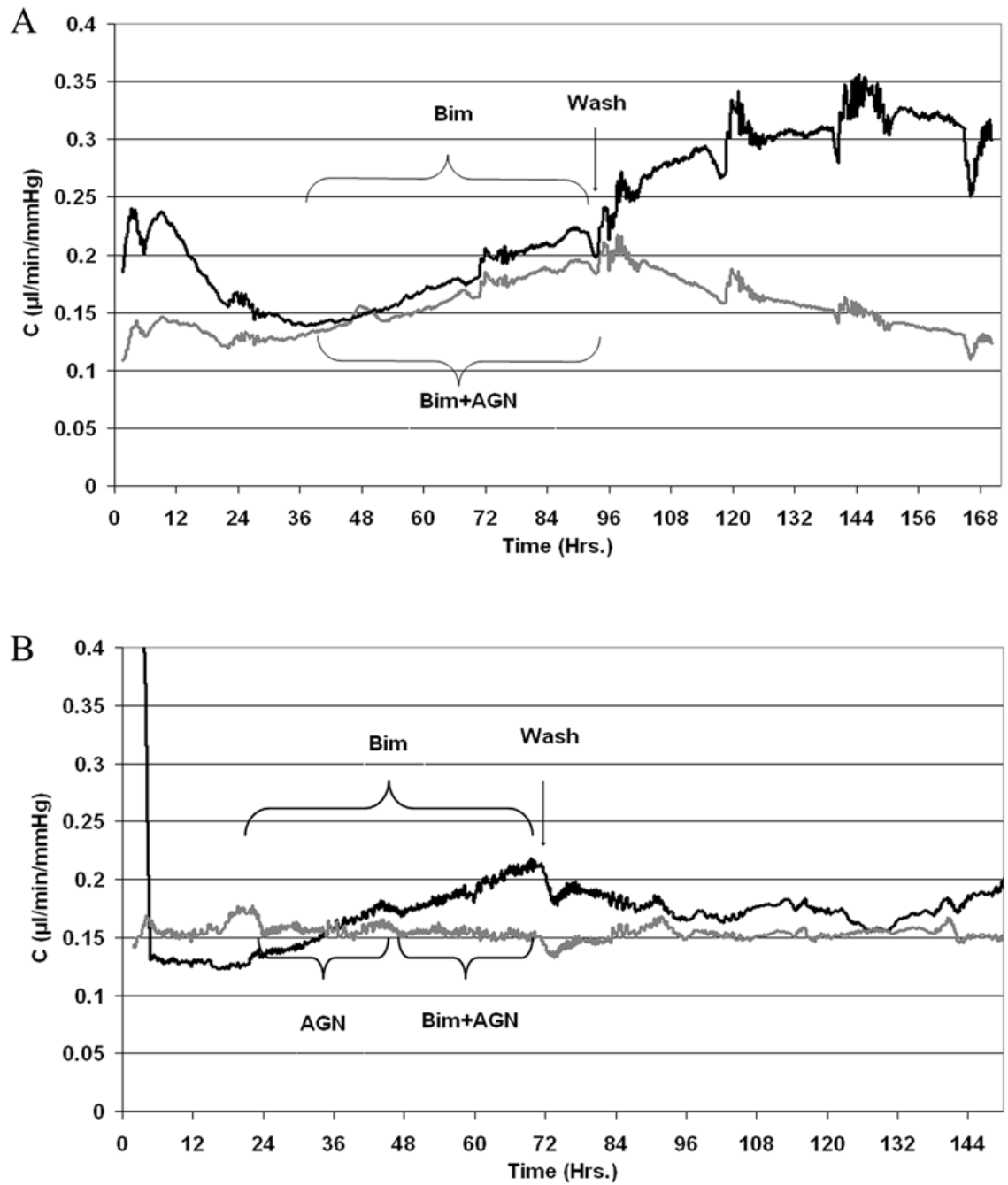


Figure 2. Facility traces of human anterior segment pairs treated with bimatoprost

After stable baseline facilities in both segment pairs were established, chambers were exchanged with medium containing $1 \mu\text{M}$ bimatoprost (BIM, black traces) or bimatoprost plus $30 \mu\text{M}$ of the prostamide antagonist, AGN211334 (AGN, gray traces). AGN 211334 was administered in one of two ways: contralateral segments were exposed to both compounds at the same time (panel A), or control segments were first pretreated with AGN 211334 and then 24 hours later were treated with AGN plus bimatoprost (panel B). Shown are representative traces of data shown in table 3.

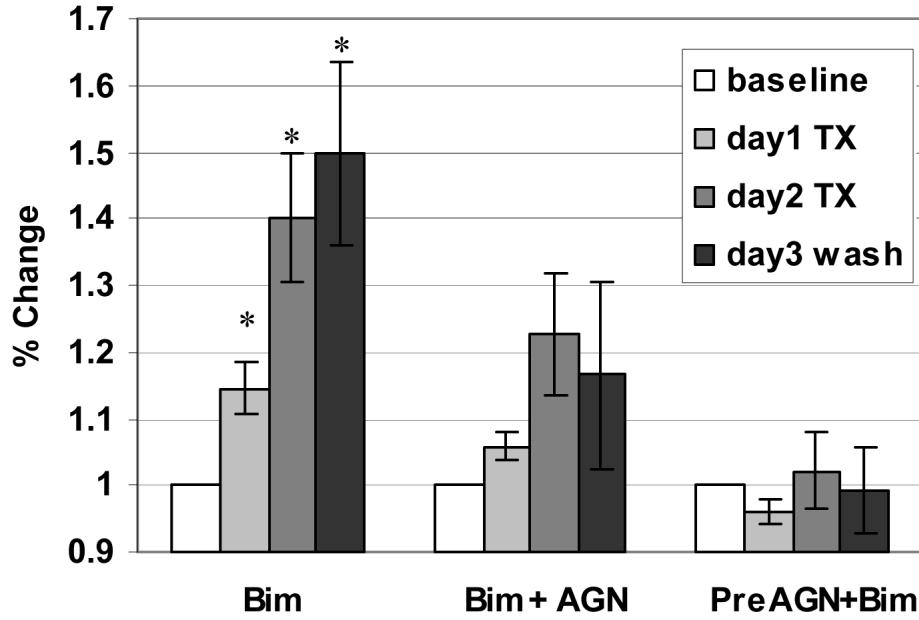


Figure 3. Summary of results showing effects of bimatoprost and/or AGN 211334 treatment on outflow facility of human anterior segments in organ culture

Data are expressed as mean (\pm SEM) per cent of baseline outflow facilities for comparisons between groups. Bimatoprost (BIM) treatment, significantly increased outflow facility by 14% after 24 hours (day1, $p=0.001$) and 40% after 48 hours (day2, $p=0.0002$). After chamber exchange with fresh medium (wash), average outflow facility measured 49% above original baseline ($p=0.001$). For contralateral anterior segment controls, co-administration of bimatoprost with AGN 211334 (BIM+AGN) resulted in an outflow facility that was 6% above baseline by 24 hours ($p=0.02$) and 23% by 48 hours ($p=0.03$). Following washout of drugs, outflow facility was 17% above baseline ($p=0.3$). For the anterior segments preincubated with AGN 211334, facility decreased 4% with AGN 211334 alone ($p=0.04$), increased by 2% after adding bimatoprost to AGN ($p=0.3$), and were 1% less than baseline after wash ($p=0.5$).

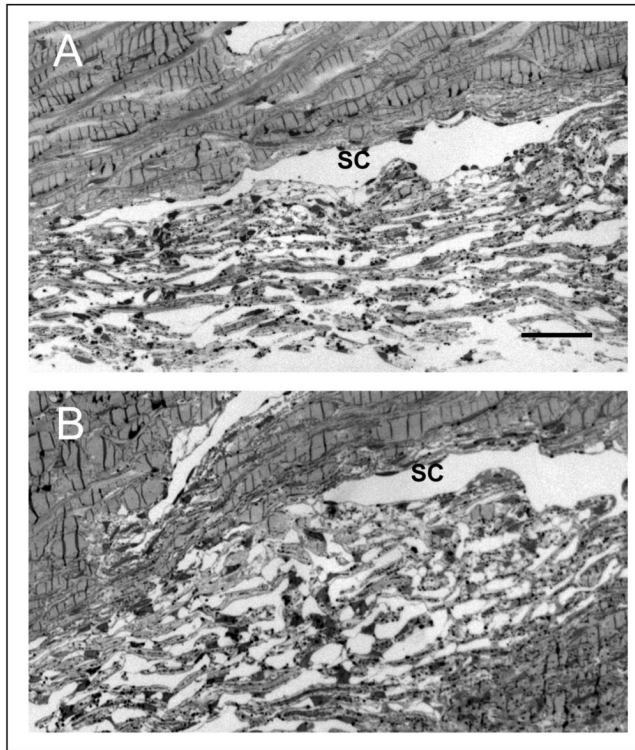


Figure 4. Histological evaluation of conventional drainage tissues following drug treatment in organ culture

Shown are toluidine blue-stained, semi-thin sections from the anterior segment pair shown in panel B of figure 2. One anterior segment (Panel A, #157) was treated with 1 μ M bimatoprost (BIM), while the contralateral segment (Panel B, #158) was first pretreated with AGN 211334 and then treated with 30 μ M AGN 211334 plus 1 μ M BIM. (SC=Schlemm's canal; bar=100 μ m).

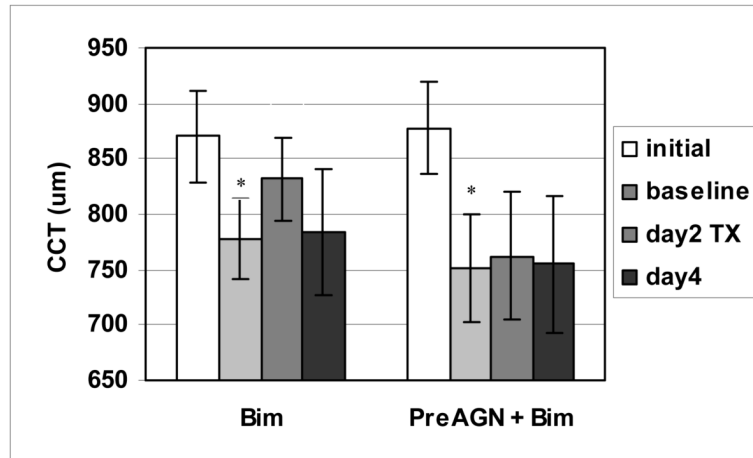


Figure 5. Summary of effects of bimatoprost treatment on central corneal thickness (CCT) measurements of human anterior segments in organ culture

Initial average CCT at the start of perfusion was $870 \pm 41 \mu\text{m}$ and $878 \pm 41 \mu\text{m}$ for bimatoprost treated (BIM) and bimatoprost plus AGN 211334 treated (*preAGN+BIM*) anterior segments, respectively. The average CCT decreased by 11% and 14% over first 24 to 72 hours of perfusion for BIM and *preAGN+BIM* anterior segments, respectively. Forty-eight hours after treatment with BIM, average CCT of segments increased by 7% ($p=0.015$). CCT began to return toward baseline measurements after washout of BIM. In *preAGN* segments however, BIM did not affect CCT measurements over time ($p=0.3$).

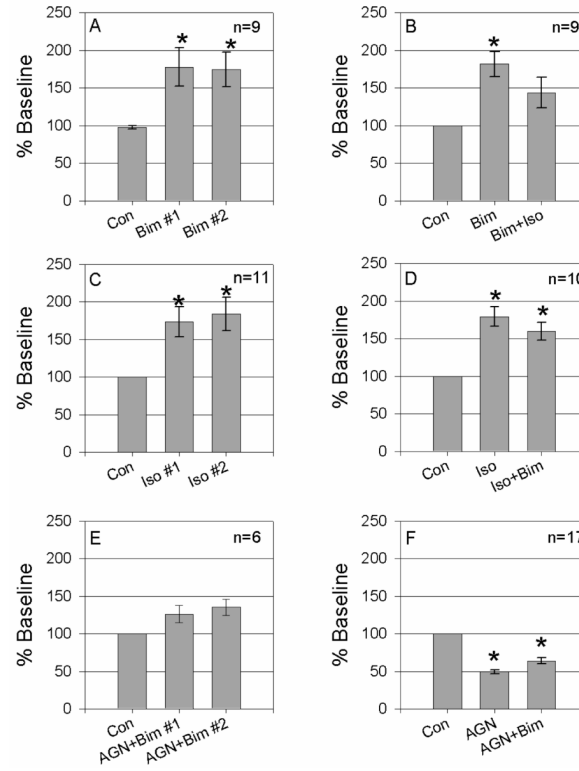


Figure 6. Bimatoprost and AGN 211334 effects on hydraulic conductivity of HTM monolayers
 Fluid flow across cell monolayers in the apical to basal direction was driven by a pressure head of 10mmHg. Prior to drug treatments, baseline hydraulic conductivities (HC) for each monolayer was measured (Con) and tested for stability after a chamber exchange with normal medium. Cells were then exposed to a single drug or drug combination by chamber exchange. Panel A shows the effect of two sequential treatments with bimatoprost (1 μ M, Bim, $p=0.01$ and $p=0.008$ for Bim #1 and Bim #2, respectively). Panel B shows effects of Bim alone or in combination with Isoproterenol (1 μ M, Bim, $p=0.001$ and $p=0.06$ for Bim and Iso+Bim, respectively). Panel C shows the results of two sequential Iso treatments ($p=0.004$ and $p=0.004$ for Iso #1 and Iso #2, respectively). Panel D shows the effects of Iso and Bim treatments in reverse order of that shown in panel B ($p=0.0002$ and $p=0.0008$ for Iso and Iso+Bim, respectively). Panel E summarizes results when AGN 211334 (30 μ M, AGN) and Bim are used in combination ($p=0.07$ and $p=0.02$ for AGN+Bim #1 and AGN+Bim #2, respectively). Panel F shows effects of AGN alone or in combination with Bim ($p=1 \times 10^{-12}$ and $p=2 \times 10^{-8}$ for AGN and AGN+Bim, respectively). Asterisks (*) indicate a significant difference between the experimental and the control at $p<0.01$.

Table 1

Antagonist activity of AGN 211334 at prostamide receptors in the feline iris and at human recombinant prostanoid receptors.

Prostanoid Receptor	Antagonist K_b (nM) for AGN 211334
Prostamide	236
DP	Inactive
EP ₁	Inactive
EP ₂	Inactive
EP ₃	Inactive
EP ₄	37,048
FP	Inactive
IP	Inactive
TP	16

Table 3
Summary of facility measurements, before and after drug treatments

Donor	ID	Drug Tx	Co ($\mu\text{l}/\text{min}/\text{mmHg}$)	D1	D2	Wash
1	163	B	0.11	0.13	0.23	0.26
2	160	B	0.09	0.10	0.14	0.18
3	157	B	0.10	0.11	0.13	0.14
4	156	B	0.13	0.13	0.14	0.15
5	150	B	0.13	0.18	0.20	0.19
6	148	B	0.51	0.54	0.54	0.53
7	145	B	0.17	0.19	0.21	0.20
9	140	B	0.16	0.17	0.22	0.28
10	137	B	0.17	0.21	0.21	0.19
11	135	B	0.19	0.21	0.28	0.28
	Mean\pmSE		0.18\pm0.04	0.20\pm0.04	0.23\pm0.04	0.24\pm0.04
7	146	AB	0.13	0.14	0.19	0.20
8	144	AB	0.19	0.21	0.24	0.23
9	139	AB	0.16	0.16	0.18	0.16
10	138	AB	0.50	0.51	0.51	0.44
	Mean\pmSE		0.24\pm0.09	0.26\pm0.09	0.28\pm0.08	0.26\pm0.06
1	164	preA	0.12	0.12	0.13	0.13
2	159	preA	0.13	0.11	0.10	0.09
3	158	preA	0.09	0.09	0.10	0.10
4	155	preA	0.16	0.15	0.15	0.15
5	149	preA	0.15	0.15	0.16	0.15
6	147	preA	0.23	0.22	0.27	0.26
	Mean\pmSE		0.15\pm0.02	0.14\pm0.02	0.15\pm0.03	0.15\pm0.03

ID: identification; Tx: treatment; Cd: outflow facility in the presence of drug; D1: day1 treatment, D2: day2 treatment, B: bimatoprost treat only, AB, AGN 211334 and bimatoprost co-treatment, preA: AGN 211334 pretreatment followed by bimatoprost treatment.